Pittsburgh Interdisciplinary Mathematics Review **5** (2026), 54–80

Modeling elephant and poacher populations using the type IV functional response

Theodora Schwallie, Lawrence Seminario-Romero

(Communicated by Leonardo Finzi
Copyedited by Joseph Tracy)

Abstract

We develop and analyze a mathematical model for describing the population interactions between elephants and poachers. This model is a *high-risk, high-reward* predator-prey model in which the poachers are discouraged from hunting elephants by punitive laws, but motivated by the high profits gained from ivory. The poachers are assumed to exhibit a *type IV* functional response which allows for this high-risk, high-reward situation to be modeled. The research question aimed to be addressed with this model is to find an equilibrium point that results in the "coexistence" of elephants and poachers, and determine its long-term stability.

1. Introduction

1.1. Motivation of the problem

Over the past 100 years poachers have killed 90% of African elephants [1]. Ivory tusks are alluring as they can be turned into valuable products like jewelry, tools, and art. African elephants are sought after at a higher rate due to both males and females having two large tusks [11, p. 8]. In 1973, the Convention on International Trade in Endangered Species (CITES) convened for the first time to discuss an international regulation on the ivory trade. The 1960s and early 1970s was a time period in which there was an increase in wildlife trade, which called for a demand in regulations [11, p. 17]. The goal of CITES was to regulate trade in animal products of species that were going extinct such as African elephants [11, p. 17]. By 2016, around $5,600$ animals were classified by CITES as endangered, with varying risk level; most types of

elephants such as African are classified as "threatened with extinction" [11, p. 18]. Despite regulation efforts by CITES, poaching still remains a prevalent problem. The high price of ivory is enticing enough to tempt many poachers into illegally killing elephants. This legal and wildlife conservation problem forms the basis for motivating this body of research in which a mathematical model is formulated, analyzed, and tested in order to better understand the dynamics associated withe population interactions between elephants and poachers over the course of time.

1.2. **Type IV functional response**

In the 1950s, C. S. Holling presented his work on *functional responses* [9, p. 68], which are used for modeling the amount of prey consumed by a predator per time. These are often labeled types I, II, and III. The type I functional response assumes that the feeding rate of a predator increases at a constant rate with respect to the number of prey consumed, but in general, this is not biologically realistic due to saturation. The most commonly utilized functional response in predator-prey modeling is the type II functional response which accounts for the amount of time a predator has to search for its prey [9, p. 68]. This type of functional response is associated with *specialist* predators. The type III functional response accounts for the population density level of the prey and it is best used for describing the consumption rates of *generalist* predators [9, p. 68]. In other words, should the amount of prey fall below a certain threshold, then the predators will not notice them and instead get their food from different sources [9, p. 68].

While these two functional responses are commonly utilized in predator-prey modeling, they do not take into account a prey's ability to *defend* itself. This is where a *type IV* functional response comes into consideration [10, p. 1183]. Although elephants cannot defend themselves, laws and park rangers practically serve a similar role as a deterrent against predators [11, p. 62]. Specifically, we assume that the larger a group of elephants is, the more park rangers there will be to monitor and protect them. As a result, we have a "group defense" behavior, which allows us to utilize the type IV functional response in our proposed model.

In the next section, we will state the assumptions and formulate the model we use to describe the population levels of elephants and poachers. The model is a nonlinear system of ordinary differential equations, which contains a term corresponding to the type IV functional response. We will summarize how this functional response is formulated, and analyze the existence and stability of the model's equilibrium solutions. From there, we fit our model parameters to available data to link the mathematical results with what has been observed empirically.

2. Formulation of the model

Our model is formulated based on the following assumptions:

(i) The "feeding rate" of the poachers follows a type IV functional response.

(ii) The elephant population exhibits logistic growth.

(iii) There is no "natural death rate" in both the elephant and poacher populations.

(iv) Poachers leave the population with a crowding term as opposed to linearly.

(v) Park rangers and laws act as the "group defense" for the elephants.

2.1. Building the base model

The construction of the model is based on the standard predator-prey model for two populations. We let E denote the elephant population, and P denote the poacher population. These equations are constructed in accordance with the balance laws. That is,

$$\begin{cases} \frac{dE}{dt} = E_{in} - E_{out} \\ \frac{dP}{dt} = P_{in} - P_{out} \end{cases} \tag{1}$$

Since the elephant population is assumed to exhibit logistic population growth [2, p. 145], we have:

$$E_{in} = mE\left(1 - \frac{E}{K}\right) \tag{2}$$

Here, m is the constant of proportionality which dictates the rate at which elephants are growing, and K is the carrying capacity for the elephants which is the maximum population size for elephants that can be sustained in a certain ecosystem.

The next term we will formulate is P_{out}. As argued by Deng et al. [5, p. 27], we want a model that does not give rise to the *Rosenzweig enrichment paradox*, which arises if P_{out} is strictly linear. One way to avoid this is to introduce density-dependence in the poacher population, and mathematically, this is given by:

$$P_{out} = sP + nP^2 \tag{3}$$

Here, s is the rate at which poachers leave the population and n is the crowding rate at which poachers leave.

We will next focus on formulating E_{out} and P_{in}, and something worth noting is that P_{in} is related to E_{out} by some scalar, e. In other words, $P_{in} = eP_{out}$ where $0 < e < 1$ is the birth-to-consumption rate, which tells us how many new poachers arise for each elephant killed. To formulate these terms, we will adopt a model given by Köhnke et al [8]. Here, we have that:

$$\begin{cases} E_{out} = f(E)P \\ P_{in} = eE_{out} \end{cases} \tag{4}$$

The term $f(E)$ denotes the type IV functional response, which we will formulate in the next subsection. As a result, we now have the following nonlinear system of ODEs for our base model:

$$\begin{cases} \frac{dE}{dt} &= mE\left(1 - \frac{E}{K}\right) - f(E)P \\ \frac{dP}{dt} &= ef(E)P - sP - nP^2 \end{cases} \tag{5}$$

The next section develops the type IV functional response $f(E)$, and this is done by splitting the poacher population P into two sub-populations: poachers who search for elephants, and poachers that handle the ivory.

2.2. **Developing the functional response**

A searching poacher is one who hunts and kills elephants, while a handling poacher is one who processes and sells the ivory. Therefore, only the searching poachers would actively pose a threat to the elephants. Let P_S be the searching population, and P_H be the handing population. Here, $P = P_S + P_H$ as all the poachers can be found by summing the two subgroups. Köhnke et al. [8, p. 2] propose the following model for this situation:

$$\begin{cases} \frac{dP_S}{dt} &= -\beta g(E)P_S + \gamma P_H \\ \frac{dP_H}{dt} &= \beta g(E)P_S - \gamma P_H \end{cases} \tag{6}$$

Here, $\beta g(E)$ is the rate that searching poachers turn into handling poachers, with $g(E)$ being the rate of a successful catch and kill of an elephant, and γ is the half-saturation rate [8, p. 2]. We can assume that the timescales of E and P are sufficiently small compared to P_S and P_H. By our assumption, $E = E(0)$ and $P = P(0)$ [8, p. 7]. Rewriting the right-hand side of P_S, we can obtain an equivalent expression for $\frac{dP_S}{dt}$:

$$\frac{dP_S}{dt} = -\left(\beta g(E) + \gamma\right)\left(P_S - \frac{\gamma P_H}{\beta g(E) + \gamma}\right) \tag{7}$$

From (7), a stationary solution for P_S is:

$$P_S^* = \frac{\gamma P_H}{\beta g(E) + \gamma} \tag{8}$$

Now, we can assume that predation only relies on searching individuals, because the poachers who are handling do not contribute to predation from the population as they do not search and kill elephants. Then, we get from [8, p. 2] that:

$$f(E)P = \beta g(E) P_S^* = \frac{\beta\gamma P_H g(E)}{\beta g(E) + \gamma} \tag{9}$$

which is a steady-state. Köhnke et al. [8, p. 4] proposed that group defense dependent on the catch rate is given by:

$$g(E) = \frac{E}{1 + (\frac{E}{C})^\nu} \tag{10}$$

In this catch rate, we will assume that $\nu < 1$ as this happens when species have group defense [8, p. 2]. We also need for $C < K$, otherwise we would get a type II functional response [8, p. 4]. We will refer to C as the *critical defense value*. Plugging in Equation (10) into Equation (9) give us:

$$f(E)P = \frac{\beta\gamma PE}{\gamma + \beta E + \gamma(\frac{E}{C})^\nu}$$

To further simplify this expression, we can let τ be handling time, which will mean that $\tau = \frac{1}{\gamma}$. As a result, we have that:

$$f(E)P = \frac{\beta EP}{1 + \beta\tau E + (\frac{E}{C})^\nu} \tag{11}$$

From Equation (11), we can see that the expression for the type IV functional response is given by

$$f(E) = \frac{\beta E}{1 + \beta\tau E + \left(\frac{E}{C}\right)^\nu},$$

which aligns with the expression provided by Líznarová and Pekár [10, p. 1184]. In their work, they developed a type IV functional response for spiders and their prey. We should note that their functional response expression utilized $\nu = 2$ [10, p. 1184].

2.3. **Proposed model and nondimensionalization**

Substituting Equation (11) into (5), gives us our proposed model:

$$\begin{cases} \frac{dE}{dt} &= mE\left(1-\frac{E}{K}\right) - \frac{\beta EP}{1+\beta\tau E+(\frac{E}{C})^{\nu}} \\ \frac{dP}{dt} &= \frac{e\beta EP}{1+\beta\tau E+(\frac{E}{C})^{\nu}} - (sP+nP^2) \end{cases} \tag{12}$$

A summary of the model's parameters can be found in Table 1.

Parameter	Dimension (Units)	Meaning
m	time^{-1}	intrinsic growth rate
K	elephants	carrying capacity
γ	$\text{elephants} \cdot \text{time}^{-1} \cdot \text{poachers}^{-1}$	processing rate
β	$\text{time}^{-1} \cdot \text{poachers}^{-1}$	search rate
e	$\text{poachers}\cdot\text{elephants}^{-1}$	conversion rate
s	time^{-1}	linear poacher removal
n	$\text{time}^{-1}\cdot \text{poachers}^{-1}$	crowding poacher removal
C	elephants	critical defense value
ν	unitless	scaling parameter
τ	$\text{time} \cdot \text{poachers} \cdot \text{elephant}^{-1}$	handling time; inverse of γ

Table 1: Model parameters. These will be chosen and fitted later on.

Since our model has nine parameters, we will proceed to *nondimensionalize* it. This is a process in which a choice of re-scaling is given to the independent and dependent variable [9, p. 31]. By nondimensionalizing our model, we will be able to cut down on the number of parameters, which in turn makes the analysis more feasible. [9, p. 31]. We use the following choice of rescaling adapted from Deng et al [5, p. 29] for our variables:

$$\begin{cases} x &= \frac{E}{K} \\ y &= \frac{P}{\frac{m}{\beta}} \\ T &= mt \end{cases}$$

If we substitute these choice of rescalings into our differential equation model, we can then use algebra to obtain the dimensionless parameters. Table 2 contains the dimensionless parameters.

Dimensionless Parameter	Rescaling	Numerical Bound(s)
a	$\beta\tau K$	$a > 0$
b	$\frac{K}{C}$	$b > 1$
ν	ν	$0 < \nu < 1$
δ	$\frac{e\beta K}{m}$	$\delta > 0$
μ	$\frac{s}{m}$	$\mu > 0$
σ	$\frac{n}{\beta}$	$\sigma > 0$

Table 2: Dimensionless parameters obtained with nondimensionalization. Note that ν is dimensionless since it is a shaping parameter.

Our nondimensionalized model is given by the following system of nonlinear differential equations:

$$\begin{cases} \frac{dx}{dT} &= x\left(1 - x - \frac{y}{1+ax+b^\nu x^\nu}\right) \\ \frac{dy}{dT} &= y\left(\frac{\delta x}{1+ax+b^\nu x^\nu} - \mu - \sigma y\right) \end{cases} \tag{13}$$

3. **Analysis of the model**

3.1. **Nullcline analysis**

We utilize nullclines to conduct the first part of our analysis. The x-nullclines are curves in the xy-plane where $\frac{dx}{dT} = 0$, and the y-nullclines are curves in the xy-plane where $\frac{dy}{dT} = 0$ [2, p. 478]. A point of intersection between an x and y-nullcline is an equilibrium point in the model [2, p. 479]. Equilibrium points are steady-state solutions, and these can provide us with information associated with plausible long-term dynamics predicted by the model [2, p. 5]. In our model, the x-nullclines are given by

$$x = 0 \tag{14}$$

$$y = (1 - x)(1 + ax + b^\nu x^\nu), \tag{15}$$

and the y-nullclines are given by

$$y = 0 \tag{16}$$

$$y = \frac{\delta x}{\sigma(1 + ax + b^\nu x^\nu)} - \frac{\mu}{\sigma} \tag{17}$$

For convenience, we will refer to the nontrivial x-nullcline given by Equation (15) as $y = f(x)$, and the nontrivial y-nullcline given by equation (17) as $y = g(x)$. The following theorem summarizes some key properties of f and g. We provide proofs for properties (5)-(6) since properties (1)-(4) are trivial.

Theorem 3.1. *Suppose that $\sigma > 0$, $\delta > 0$, $0 < a$, $\nu < 1$, $b > 1$. Then,*

(1) $f(0) = 1$

(2) $f(1) = 0$

(3) $f(x) > 0$ *on* $(0, 1)$

(4) $g(0) = -\frac{\mu}{\sigma}$

(5) $g(x) < \frac{\delta}{\sigma a} - \frac{\mu}{\sigma}$ *for all* $x > 0$.

(6) g *is increasing for all* $x > 0$.

Proof. To prove (5), we can note that

$$\lim_{x\to\infty} g(x) = \lim_{x\to\infty} \left(\frac{\delta x}{\sigma(1 + ax + b^\nu x^\nu)} - \frac{\mu}{\sigma} \right) = \frac{\delta}{\sigma a} - \frac{\mu}{\sigma}$$

This means that $y = g(x)$ has a horizontal asymptote given by $y = \frac{\delta}{\sigma a} - \frac{\mu}{\sigma}$. Now, we will show that $g(x) < \frac{\delta}{\sigma a} - \frac{\mu}{\sigma}$ for all $x > 0$. Suppose by contradiction, there exists an $x > 0$ such that $g(x) \geq \frac{\delta}{\sigma a} - \frac{\mu}{\sigma}$. We then have:

$$\frac{\delta x}{\sigma(1 + ax + b^\nu x^\nu)} - \frac{\mu}{\sigma} \geq \frac{\delta}{\sigma a} - \frac{\mu}{\sigma},$$

or equivalently,

$$\frac{\delta x}{\sigma(1 + ax + b^\nu x^\nu)} \geq \frac{\delta}{\sigma a}.$$

We can cancel the $\frac{\delta}{\sigma}$ from both sides of the inequality to obtain $\frac{x}{1+ax+b^\nu x^\nu} \geq \frac{1}{a}$, which is equivalent to $ax \geq 1 + ax + b^\nu x^\nu$. This inequality simplifies down to $1 + b^\nu x^\nu \leq 0$, which is a contradiction since we assume that b, ν, $x > 0$.

To prove (6), we can use the derivative of g:

$$g'(x) = \frac{\sigma\delta + (1-\nu)\delta\sigma b^\nu x^\nu}{(\sigma + \sigma a x + \sigma b^\nu x^\nu)^2} = \frac{p(x)}{q(x)}$$

It is clear that by construction $q(x) > 0$. Since $p(x) = \sigma\delta + (1-\nu)\delta\sigma b^\nu x^\nu$, our parameter constraints along with $x > 0$ implies that $p(x) > 0$. This means that $g'(x) > 0$, which implies that $y = g(x)$ is increasing. □

Theorem 3.2. *$g(1) > 0$ if and only if $\delta - \mu a > \mu(1 + b^\nu)$.*

Proof. Let's start by noting that $g(1) = \frac{\delta}{\sigma(1+a+b^\nu)} - \frac{\mu}{\sigma}$. Then $g(1) > 0$ is equivalent to $\frac{\delta}{\sigma(1+a+b^\nu)} - \frac{\mu}{\sigma} > 0$, or equivalently, $\frac{\delta}{1+a+b^\nu} > \mu$. This, in turn, is equivalent to $\delta - \mu a > \mu(1 + b^\nu)$. Therefore, the biconditional statement holds. □

The result described by Theorem 3.2 in essence establishes what condition is needed to guarantee the existence of *positive* equilibrium points. These are steady-state solutions in which $0 < x^* < 1$ and $y^* > 0$. Going forward, we will refer to these kind of equilibrium points as *coexistence equilibria*. As a small remark, the only reason why we have $x \leq 1$ is that $x = 1$ represents the "re-scaled" carrying capacity value of elephants. Note that if Theorem 3.2 is false, then we have that $\delta - \mu a \leq \mu(1 + b^\nu)$, which would imply that $g(1) \leq 0$. Since g is increasing for all $x > 0$, we would have that $g(x) < 0$ for all $x \in [0, 1]$. As a result, this would also imply that there is no coexistence equilibria on $[0, 1]$, because $f(x) > 0$.

3.2. **Existence of equilibria**

Using our nullclines, along with the properties described in Theorems 3.1 and 3.2, we can now identify equilibria. Since we are modeling population dynamics, we restrict ourselves to equilibria in which $x, y \geq 0$. Let's start by solving for the *trivial* equilibrium points. One of these is $(0, 0)$, which is the point of intersection between the x-nullcline $x = 0$ and the y-nullcline $y = 0$. This equilibrium is known as the *extinction equilibrium*, which is the steady state in which there is an absence of both elephants and poachers. Another equilibrium point is $(1, 0)$, which is the point of intersection between the x-nullcline $y = f(x)$ and the y-nullcline $y = 0$ as described in Theorem 3.1. This equilibrium is known as the *carrying capacity equilibrium*, which is the steady state in which the elephant population will be at carrying capacity due to an absence of poachers. Finding the *nontrivial* equilibrium points (or coexistence equilibria) requires a formal mathematical argument.

Theorem 3.3. *If $\delta - \mu a > \mu(1 + b^{\nu})$, then there will be at least one coexistence equilibrium point.*

Proof. By construction, the x-nullcline given by $y = f(x)$ and the y-nullcline given by $y = g(x)$ are continuous on $[0, 1]$. We know from Theorem 3.1 that $f(0) = 1$, $f(1) = 0$, and $g(0) = -\frac{\mu}{\sigma} < 0$. We also know from *Theorem 3.2* that $g(1) > 0$. So, $f(0) > g(0)$ and $g(1) > f(1)$. By the *Intermediate Value Theorem*, there exists at least one $x^* \in (0, 1)$ such that $f(x^*) = g(x^*)$. Let $y^* = f(x^*)$. Then Theorem 3.1 implies that $y^* \in (0, \frac{\delta}{\sigma a} - \frac{\mu}{\sigma})$. Therefore, there is at least one coexistence equilibrium point (x^*, y^*). □

Figure 1 provides an illustration of what the nullclines look like, and where they intersect in Quadrant I of the xy-plane. However, note that the values chosen for the parameters are arbitrary within the bounds of what is feasible for those parameters.

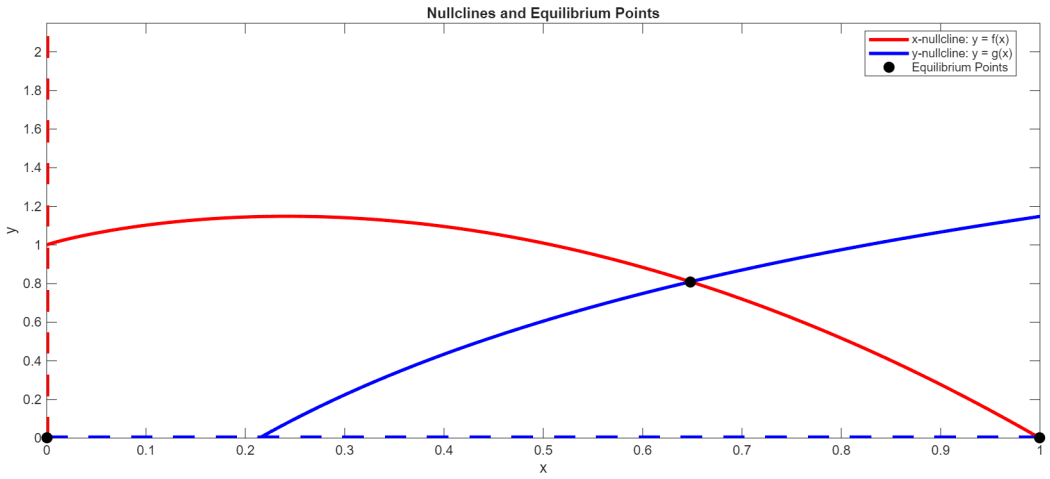

Figure 1: Nullclines and equilibrium points. Here, $a = 0.95$; $b = 1.01$; $\nu = 0.89$; $\delta = 0.3$; $\mu = 0.044$; $\sigma = 0.05$. The red dashed line is the x-nullcline $x = 0$, and the blue dashed line is the y-nullcine $y = 0$.

3.3. **Stability of the Equilibria**

Since our model is of the form

$$\begin{cases} \frac{dx}{dT} &= \mathcal{F}(x, y) \\ \frac{dy}{dT} &= \mathcal{G}(x, y) \end{cases}$$

we can utilize the Jacobian matrix to classify its stability [7, p. 207]:

$$J(x,y) = \begin{bmatrix} \mathcal{F}_x(x,y) & \mathcal{F}_y(x,y) \\ \mathcal{G}_x(x,y) & \mathcal{G}_y(x,y) \end{bmatrix}$$

The entries in this matrix are:

$$\mathcal{F}_x(x,y) = 1 - 2x - \frac{y}{1+ax+b^\nu x^\nu}\left(1 - \frac{ax+\nu b^\nu x^\nu}{1+ax+b^\nu x^\nu}\right) \tag{18}$$

$$\mathcal{F}_y(x,y) = -\frac{x}{1+ax+b^\nu x^\nu} \tag{19}$$

$$\mathcal{G}_x(x,y) = \frac{\delta y\,(1+(1-\nu)b^\nu x^\nu)}{(1+ax+b^\nu x^\nu)^2} \tag{20}$$

$$\mathcal{G}_y(x,y) = \frac{\delta x}{1+ax+b^\nu x^\nu} - \mu - 2\sigma y \tag{21}$$

We can plug in the x and y-values of our equilibria into our Jacobian matrix, and then classify their stability using the signs of the determinant ($\mathcal{D}$) and trace ($\mathcal{T}$) of the matrix in accordance with the following definition.

Definition 3.4. [2, p. 351] An equilibrium point is:

(i) A *saddle point* when $\mathcal{D} < 0$.

(ii) *Locally stable* if $\mathcal{D} > 0$ and $\mathcal{T} < 0$.

(iii) *Unstable* if $\mathcal{D} > 0$ and $\mathcal{T} > 0$.

3.3.1 Stability of the extinction equilibrium

The Jacobian matrix at $(0,0)$ is given by:

$$J(0,0) = \begin{bmatrix} 1 & 0 \\ 0 & -\mu \end{bmatrix} \tag{22}$$

Since this is a 2×2 *diagonal* matrix, the determinant is given by the product of the diagonal entries [**?**]. So, $\mathcal{D} = -\mu$, and since $\mu > 0$, we have then that $\mathcal{D} < 0$. As a result, $(0,0)$ is a saddle point in accordance with Definition 3.4. This means that $(0,0)$ is unstable. That is, there is no expectation that both the elephant and poacher populations will vanish.

3.3.2 Stability of the carrying capacity equilibrium

The Jacobian matrix at $(1,0)$ is given by:

$$J(1,0) = \begin{bmatrix} -1 & -\frac{1}{1+a+b^\nu} \\ 0 & \frac{\delta}{1+a+b^\nu} - \mu \end{bmatrix} \tag{23}$$

Since this is a 2×2 *upper triangular* matrix, the determinant is given by the product of the diagonal entries [?]. So, $\mathcal{D} = -\left(\frac{\delta}{1+a+b^\nu} - \mu\right)$. Since we are assuming that $\delta - \mu a > \mu(1+b^\nu)$, this would imply that $\frac{\delta}{1+a+b^\nu} - \mu > 0$, which means that $\mathcal{D} < 0$. As a result, $(1,0)$ is a saddle point in accordance with Definition 3.4. Similar to the extinction equilibrium, our model predicts that $(1,0)$ is unstable, assuming that the condition $\delta - \mu a > \mu(1+b^\nu)$ is true.

If the condition $\delta - \mu a > \mu(1+b^\nu)$ is false, that is, $\delta - \mu a \leq \mu(1+b^\nu)$, then this would imply $\frac{\delta}{1+a+b^\nu} - \mu \leq 0$, which would mean that $\mathcal{D} \geq 0$ and $\mathcal{T} < 0$. Furthermore, there are only two possible steady-state solutions: $(0,0)$ and $(1,0)$. If $\mathcal{D} = 0$, then we cannot directly classify the stability of $(1,0)$, and we can turn to numerical analysis to gain insights about the stability in this case. The parameter space that would cause $\mathcal{D} = 0$ is not relevant to our applications, that we can say that $\mathcal{D} > 0$ in practice. As a result, $(1,0)$ would be locally stable in accordance with Definition 3.4. An implication of this is that conditions are favorable for the elephant population to persist at carrying capacity, with poaching activity becoming completely eliminated. This, by all practical purposes, is the most desired outcome in terms of conservation efforts. Nevertheless, it is still possible for poaching activities to exists despite the strictness of hunting regulations. For this reason, we want to at least investigate what the stability corresponding to the coexistence equilibrium point (x^*, y^*) could possibly be.

3.3.3 Stability of the coexistence equilibrium

Since our model is also of the form

$$\begin{cases} \frac{dx}{dT} = xF(x,y) \\ \frac{dy}{dT} = yG(x,y) \end{cases} \tag{24}$$

we can use a special form of the Jacobian matrix to classify the stability of $(x^*, y^*) \in (0,1) \times \left(0, \frac{\delta}{\sigma a} - \frac{\mu}{\sigma}\right)$ [3, p. 130]:

$$\begin{bmatrix} j_{11} & j_{12} \\ j_{21} & j_{22} \end{bmatrix} = \begin{bmatrix} x^* F_x(x^*, y^*) & x^* F_y(x^*, y^*) \\ y^* G_x(x^*, y^*) & y^* G_y(x^*, y^*) \end{bmatrix} \tag{25}$$

We will note for convenience that $F(x,y) = 1 - x - \frac{y}{1+ax+b^\nu x^\nu}$, and $G(x,y) = \frac{\delta x}{1+ax+b^\nu x^\nu} - \mu - \sigma y$. Here, the entries of our Jacobian matrix at (x^*, y^*) are as follows:

$$j_{11} = x^* \left(-1 + \frac{y^* \left(a + \nu b^\nu (x^*)^{\nu-1}\right)}{(1 + ax^* + b^\nu (x^*)^\nu)^2} \right) \tag{26}$$

$$j_{12} = -\frac{x^*}{1 + ax^* + b^\nu x^{*\nu}} \tag{27}$$

$$j_{21} = y^* \left(\frac{\delta + (1-\nu)\delta b^\nu (x^*)^\nu}{(1 + ax^* + b^\nu (x^*)^\nu)^2} \right) \tag{28}$$

$$j_{22} = -\sigma y^* \tag{29}$$

We can observe by the construction of the formulations for j_{12} and j_{22} that these entries are negative for any coexistence equilibrium point (x^*, y^*). Furthermore, the j_{21}-entry is positive for any coexistence equilibrium point (x^*, y^*), because our parameters are positive and $0 < \nu < 1$. With these items in mind, we can input the signs of those entries into $J(x^*, y^*)$:

$$J(x^*, y^*) = \begin{bmatrix} j_{11} & (-) \\ (+) & (-) \end{bmatrix} \tag{30}$$

We will employ the following lemma from [**?**] to investigate the sign of j_{11}.

Lemma 3.5. *Let $y = f(x)$ be the nontrivial x-nullcline from (24). Then j_{11} has the same sign as $f'(x^*)$. That is, $j_{11} = -j_{12} f'(x^*)$ where x^* is the x-value of the coexistence equilibrium point.*

Proof. Since $y = f(x)$ is an x-nullcline, we have that $F(x, f(x)) = 0$. Let us set $Q(x) = F(x, f(x))$. Then $\frac{dQ}{dx} = \frac{dF}{dx}$. By the Multivariable Chain Rule, we can get:

$$\begin{aligned} \frac{dQ}{dx} &= \frac{d}{dx}[F(x, f(x))] \\ &= \frac{\partial F}{\partial x} \cdot \frac{d}{dx}[x] + \frac{\partial F}{\partial y} \cdot \frac{d}{dx}[f(x)] \\ &= \frac{\partial F}{\partial x} + \frac{\partial F}{\partial y} \cdot f'(x) \end{aligned}$$

At (x^*, y^*) we have that $\frac{\partial F}{\partial x} = j_{11}$ and $\frac{\partial F}{\partial y} = j_{12}$. Furthermore, since $Q(x) = 0$, then we know that $\frac{dQ}{dx} = 0$. At (x^*, y^*), we find that:

$$j_{11} + j_{12} \cdot f'(x^*) = 0,$$

or equivalently,

$$j_{11} = -j_{12} f'(x^*)$$

Since j_{12} is negative, we have then that j_{11} has the same sign as $f'(x^*)$. □

With Lemma 3.5, along with the fact that (x^*, y^*) exists as given by Theorem 3.3, we can utilize a graphical analysis of the x-nullcline $y = f(x)$ to determine the stability of (x^*, y^*) by examining its monotonocity at $x = x^*$. In particular, we will classify the stability of (x^*, y^*) for a specific case.

Theorem 3.6. *If the x-nullcline given by $y = f(x)$ is decreasing at $x = x^*$, then (x^*, y^*) is locally stable.*

Proof. Suppose that the x-nullcline given by $y = f(x)$ is decreasing at $x = x^*$. Then $f'(x^*) \leq 0$. By Theorem 3.5, this would mean that $j_{11} \leq 0$. So, the signs of the entries in our Jacobian matrix at (x^*, y^*) is either:

$$\begin{bmatrix} (-) & (-) \\ (+) & (-) \end{bmatrix} \text{ or } \begin{bmatrix} (0) & (-) \\ (+) & (-) \end{bmatrix}$$

In either case, we find that $\mathcal{D} > 0$ and $\mathcal{T} < 0$. Therefore, by Definition 3.4, the coexistence equilibrium point (x^*, y^*) is locally stable. □

For scenarios in which the x-nullcline given by $y = f(x)$ is *increasing* at $x = x^*$, the stability of the coexistence equilibrium depends on parameters. An analysis could be done to classify the equilibrium point, but it is beyond the scope of this paper. Nevertheless, in the next section we will present a possible outcome for the stability of (x^*, y^*) in this case through a simulation.

4. **Simulations of model**

We ran simulations with MATLAB 2024b. The inputs are parameters corresponding to the nondimensionalized version of the model. We will note that our choice of parameter values are arbitrarily selected within the bounds defined earlier in Table 2, since we are mainly interested in visually understanding the dynamics predicted by our model.

4.1. **Simulating theorem 3.6**

Suppose that we have a selection of parameters that produce a coexistence equilibrium point (x^*, y^*) in which $y = f(x)$ is decreasing at $x = x^*$. Figure 2 is an example of this case. According to Theorem 3.6, (x^*, y^*) will be locally stable, which

can be confirmed with the phase plane shown in Figure 3. We can then take things an extra step further by plotting the nondimensionalized population levels over the course of time. See Figure 4. According to this figure, a rapid rise in poaching is associated with a steady decline in the number of elephants, but not necessarily an extinction of the species. This could be potentially attributed to conservation efforts and the implementation of poaching laws, but these don't necessarily result in an steady increase in the long-term.

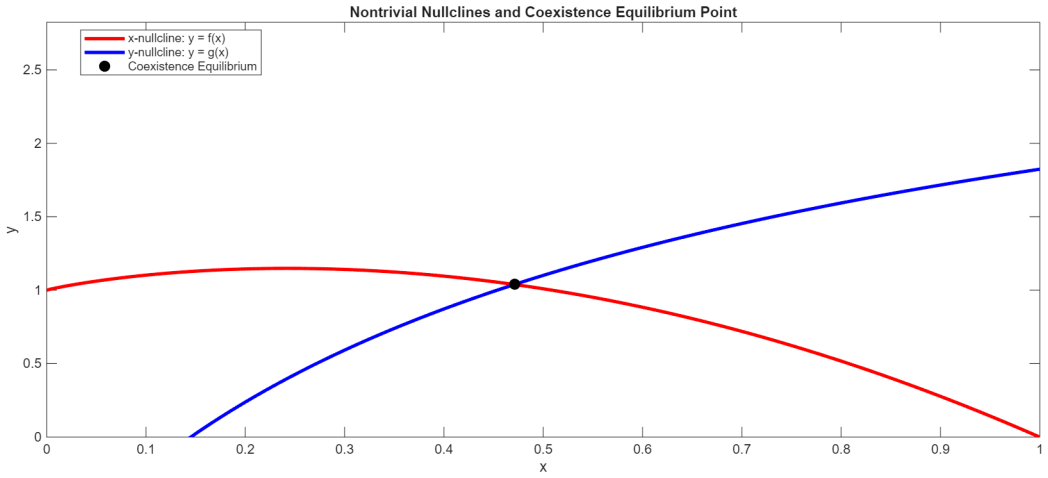

Figure 2: Nontrivial x and y-nullclines in which (x^*, y^*) falls along the portion of the x-nullcline that is decreasing. Our dimensionless parameters are: $a = 0.95$; $b = 1.01$; $\nu = 0.89$; $\delta = 0.4$; $\mu = 0.044$; $\sigma = 0.05$.

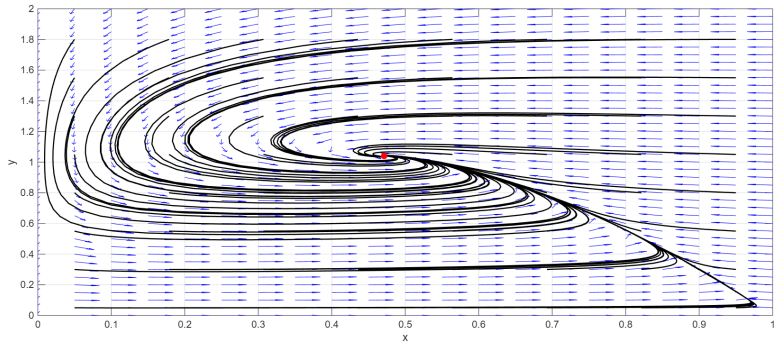

Figure 3: Phase plane showing example solutions converging to (x^*, y^*). The parameters from Figure 2 are used here.

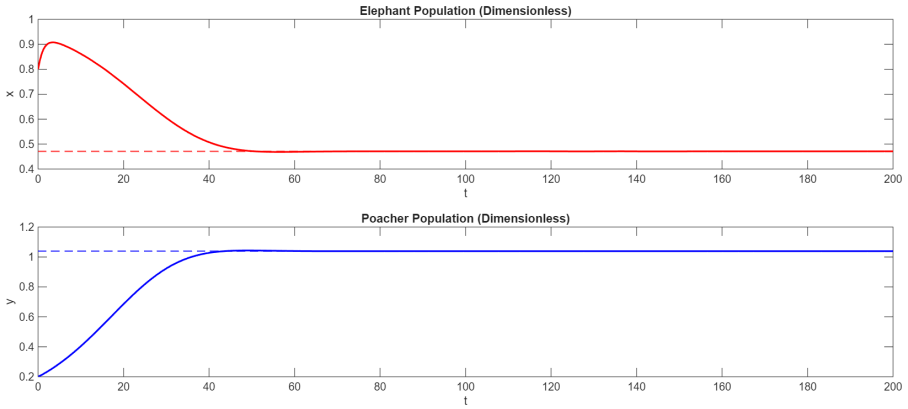

Figure 4: The nondimensionalized elephant population is initially larger than the nondimensionalized poacher population. A low number of poachers would allow for the elephant population to grow, however, so does the poacher population. Once the poachers reach a large enough population, they begin hunting down the elephants, which turn causes the elephant population to drop. Eventually, the nondimensionalized elephant population stabilizes close to 0.5, and the nondimensionalized poacher population stabilizes a little above 1. There are 200 time-steps used in this simulation. The initial conditions are given by $(x_0, y_0) = (0.8, 0.2)$. The parameters from Figure 2 are used here.

4.2. **A simulation involving non-explicit conditions**

Theorem 3.6 is in essence a *sufficient* condition for long-term stability, but it could be possible for the dynamics of our model to vary in other scenarios, for which we don't have explicit conditions. A notable instance would be the case in which a coexistence equilibrium point is on a portion of the x-nullcline given by $y = f(x)$ that is increasing. For this particular case, we would have that $f'(x^*) \geq 0$, which would imply that $j_{11} \geq 0$ due to Theorem 3.5. So, the signs of the entries in our Jacobian matrix at (x^*, y^*) is either:

$$\begin{bmatrix} (0) & (-) \\ (+) & (-) \end{bmatrix} \text{ or } \begin{bmatrix} (+) & (-) \\ (+) & (-) \end{bmatrix}$$

In the former matrix, we find that $\mathcal{D} > 0$ and $\mathcal{T} < 0$. Therefore, by Definition 3.4, the coexistence equilibrium point (x^*, y^*) would be locally stable. But, in the latter matrix, we are not able to explicitly determine the signs of $\mathcal{D}$ and $\mathcal{T}$. For this reason, we utilize MATLAB to investigate the dynamics graphically to get a sense of what *could* occur with the elephant and poacher population levels over time. See Figures 5-7. Note that we utilize the same set of parameters as before, with δ being the only changed parameter value.

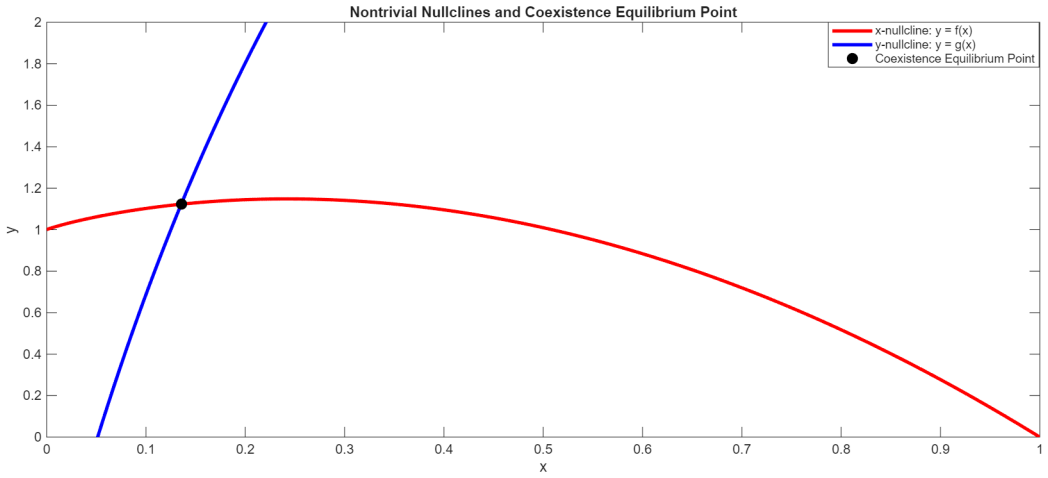

Figure 5: Nontrivial x and y-nullclines in which (x^*, y^*) falls along the portion of the x-nullcline that is increasing. Our dimensionless parameters are: $a = 0.95$; $b = 1.01$; $\nu = 0.89$; $\delta = 0.96$; $\mu = 0.044$; $\sigma = 0.05$.

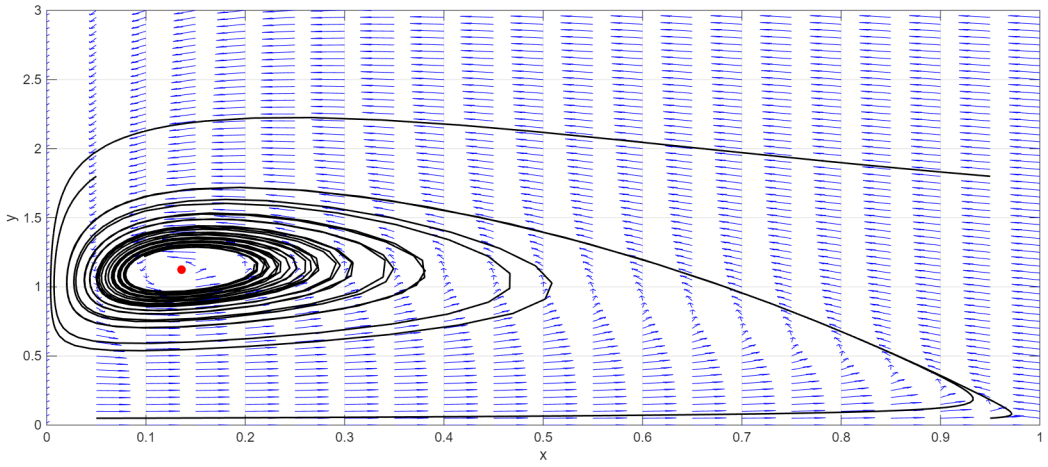

Figure 6: Phase plane showing that example solutions approaching a closed orbit around (x^*, y^*). That is, there is a limit cycle around the equilibrium point. The parameters from Figure 5 are used here.

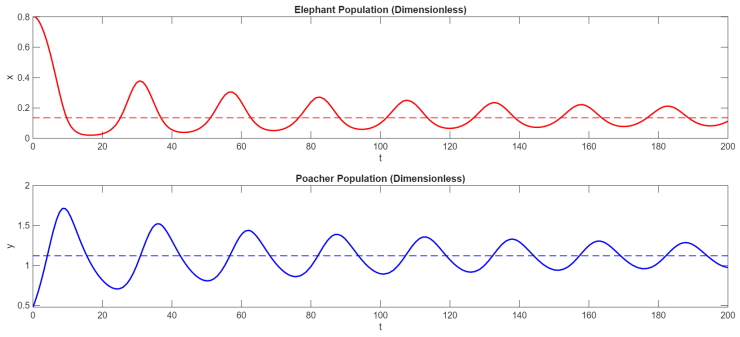

Figure 7: The nondimensionalized elephant population once again starts above the nondimensionalized poacher population. Similar to the previous simulation, the elephant population increases slightly before the poacher population grows. Then once the poacher population has grown large enough, the elephant population starts to decline. However, unlike the prior simulation where the nondimensionalized populations stabilized immediately, these nondimensionalized populations oscillate over the course of time. In other words, these dynamics are consistent with *seasonal* hunting. The initial conditions are given by $(x_0, y_0) = (0.8, 0.2)$. The parameters from Figure 5 are used here.

5. **Working with data**

Our simulations allow us to get a good idea of what will occur with the population dynamics between elephants and poachers over the course of time. This section focuses on fitting our model to available data, in order to better link the mathematical results and predictions with real life elephant-poacher interactions. In particular, we want to discuss how well our model performs with what has been observed empirically.

5.1. **Overview of the data**

To test our model's performance, we will consider the elephant population found at Kruger National Park in South Africa. In the early nineteenth century, the Kruger elephant population was reported to be abundant until high levels of poaching nearly reduced the population to extinction zero in the twentieth century [12]. Fortunately, the African elephant population in Kruger has been progressively recovering thanks to human protection efforts and is now thriving [12]. Nevertheless, the threat of poachers is still active despite all active protective measures. This scenario represents a good example of how we can apply the high-risk, high-reward component associated with our model.

We obtained data from two sources. The first data set involves the number of African elephants poached in Kruger National Park from 1980 to 2020; this data was collected by *Poaching Facts*, which is an organization dedicated to protecting endangered animals [6]. The other data set involves the elephant population levels in Kruger from 1995 to 2012; this data was collected by the *Great Elephant Census*, which conducted a continent-wide survey in 2016 on the elephant population levels across Africa [4]. For our model, we also need the number of poachers over-time. However, data on this variable is scarce since surveying individuals on poaching activity is not feasible. Furthermore, countries are reluctant to release data on poacher arrests or provide estimates on the number of active poachers. One way to work around this is that we can estimate the number of poachers over time by setting it equal to the number of elephants poached over time. The data containing these estimates is shown in Table 3.

Year	Number of Elephants	Elephant Poached (Number of Poachers)
1995	8,064	12
1996	8,320	5
1997	8,371	1
1998	8,869	2
1999	9,152	2
2000	8,356	0
2001	9,276	0
2002	10,459	0
2003	11,672	0
2004	11,483	0
2005	12,467	0
2006	12,427	0
2007	13,050	0
2008	12,930	0
2009	13,573	0
2010	13,750	0
2011	14,454	0
2012	16,571	0

Table 3: Data on the Kruger elephant population from 1995 to 2012.

5.2. **First-order sensitivity analysis of the parameters**

Prior to fitting the model to data, it is important to understand which parameter variations have the largest impacts on the model. We utilized MATLAB code[1] in which we varied the model parameters, ran simulations several times, and then measured the number of poachers and elephants at the end of each simulation. These final population numbers are then plotted against the varying parameter values. See Figures 8 and 9. From Figure 8, we can observe that K (elephant carrying capacity) and C (the critical defense value) have the most significant impact on the final number of elephants, whereas the other parameters do not. Figure 9 shows trends for e, n and τ. As e (elephant to poacher conversion rate) increases, so does the end number of poachers. As n (crowding poacher removal) increases, the final number of poachers decreases. Finally, as τ (handling time) increases, the number of poachers decreases.

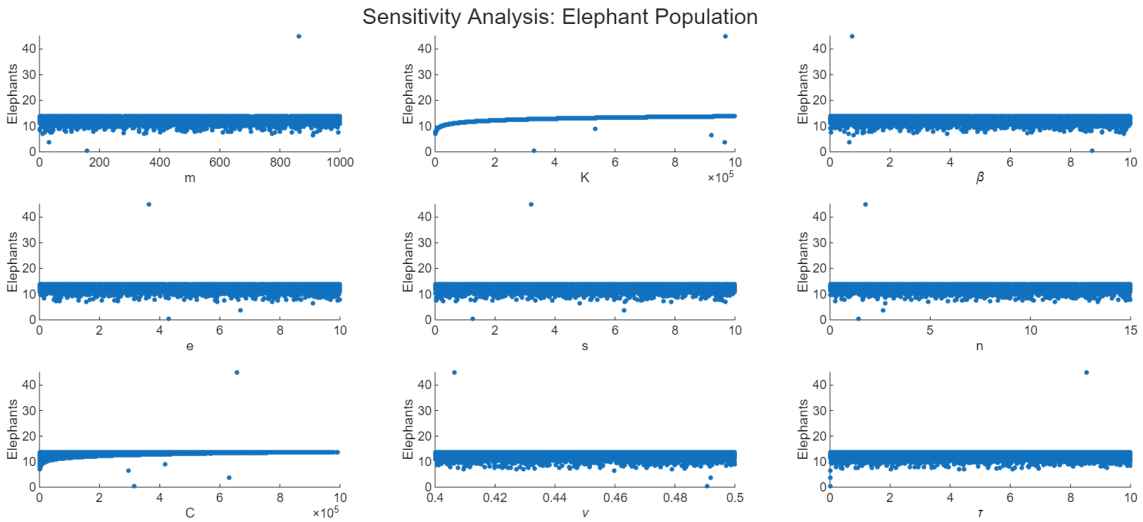

Figure 8: First-order sensitivity analysis of the model parameters on the final number of elephants.

[1]MATLAB code was adapted from *Math 397: Probabilistic Models and Methods* taught by Dr. Reginald McGee at Haverford College.

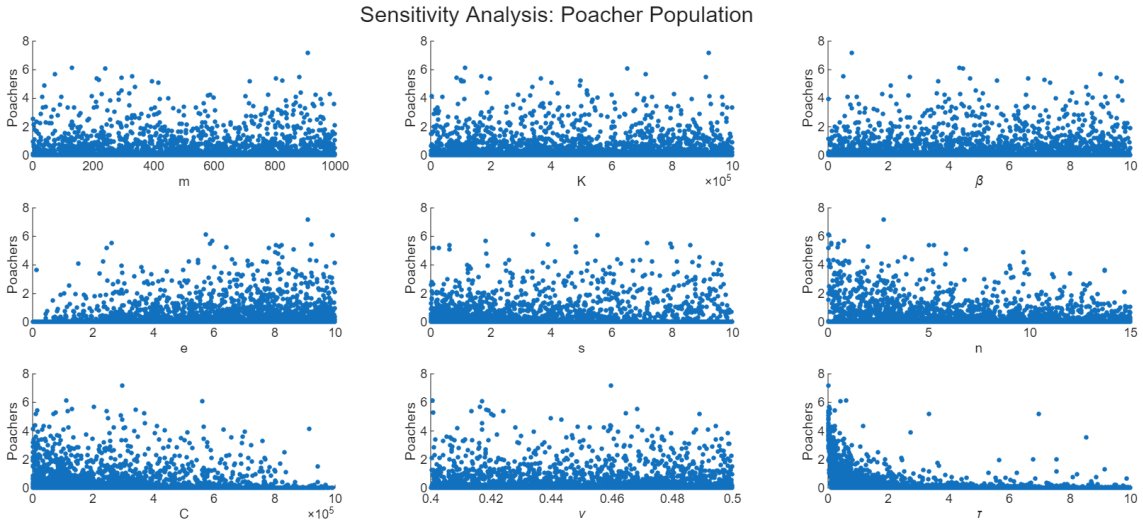

Figure 9: First-order sensitivity analysis of the model parameters on the final number of poachers.

5.3. **Fitting the model to data**

We used MATLAB[2] to fit our model to data. For each parameter, we defined a range, and specified a possible expected value. Estimating the values of the model parameters can be tricky, and we want to note that our model is very sensitive to the initial expected value of the parameter that is inputted. For these reasons, we conducted several tests with different initial guesses in order to find the best fit of the model. Then, the model takes the data, and runs the original model with our estimated parameter values to see how good of a fit it is. We then run a cost function while varying the parameters to see which values of the parameters are closest to the data. After running multiple times, the parameter values that best fit the data are saved, and the model is plotted against the best fit parameter version of the model.

Table 4 contains parameters with a reasonable fit between model and data. These parameters serve as our initial guesses when we perform fitting. The two plots from Figure 10 show a fit of the elephant population and poacher population levels over time, respectively. We will note that the two plots shown in Figure 10 are on different scales, but it is graphically evident that the model does not quite exactly fit the data points utilized.

[2]MATLAB code was adapted from *Math 382: Mathematical Modeling and Differential Equations* taught by Dr. Rebecca Everett at Haverford College.

Parameter	Initial Guess Value
m	0.5
K	15,000
β	0.0013
e	0.009
s	1.15
n	0.00025
C	7,000
ν	0.45
τ	0.5

Table 4: Initial guesses for the model parameters.

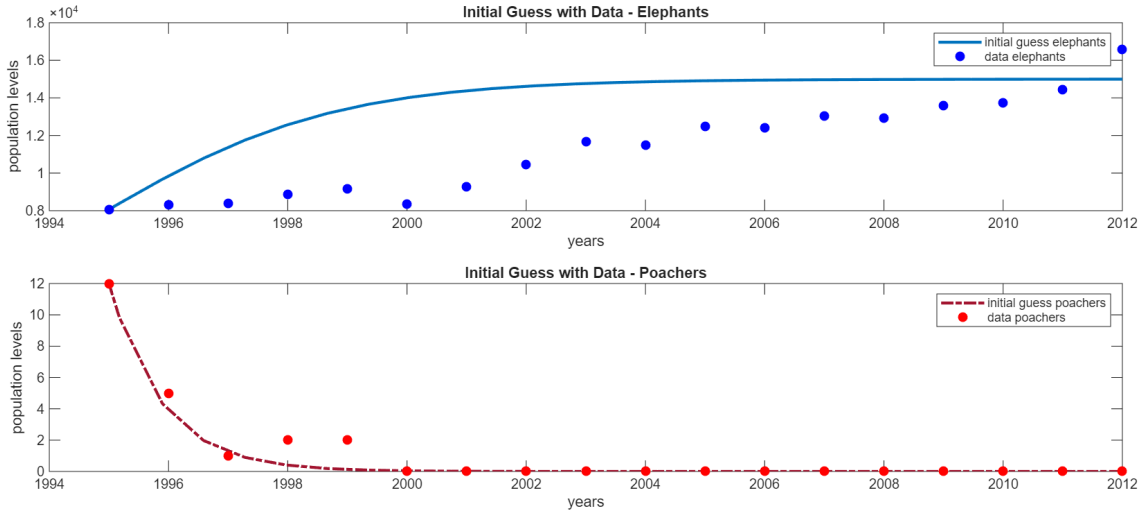

Figure 10: A fit of the elephant and poacher population data with initial guess parameters from Table 4. The poacher data in the second subplot is inferred from the elephant population over the years.

We used another MATLAB program to estimate the best-fit model parameters using constrained nonlinear least-squares optimization (**fmincon**). The sum of squared errors between the model and observed data was minimized subject to specified parameter bounds. See Table 5, as well as the two subplots shown in Figure 11. The first subplot shows that the model fits the elephant population data relatively well, which provides support for our earlier assumption of logistic growth in the elephant population. Furthermore, the second subplot shows that the model predicts a decrease in the poaching population over time, eventually reaching levels that are nearly zero. To some extent, this provides a plausible estimate of poaching activity levels for African

elephants, since, as noted earlier, such data are limited. It also provides an indication of the effectiveness of initiatives aimed at protecting African elephants in Kruger National Park; namely, the model suggests that poaching activity has been substantially reduced. We note, however, that this does not mean that poaching has been completely eliminated in Kruger, as demonstrated by the plot of the x- and y-nullclines using the *dimensionless* versions of the parameter values in Table 5. See Figure 12.

Parameter	Best Fit Value
m	0.0863
K	$33,315$
β	2.0142
e	0.0821
s	10
n	0.4825
C	$15,196$
ν	0.4
τ	0.00768

Table 5: Best fit model parameters.

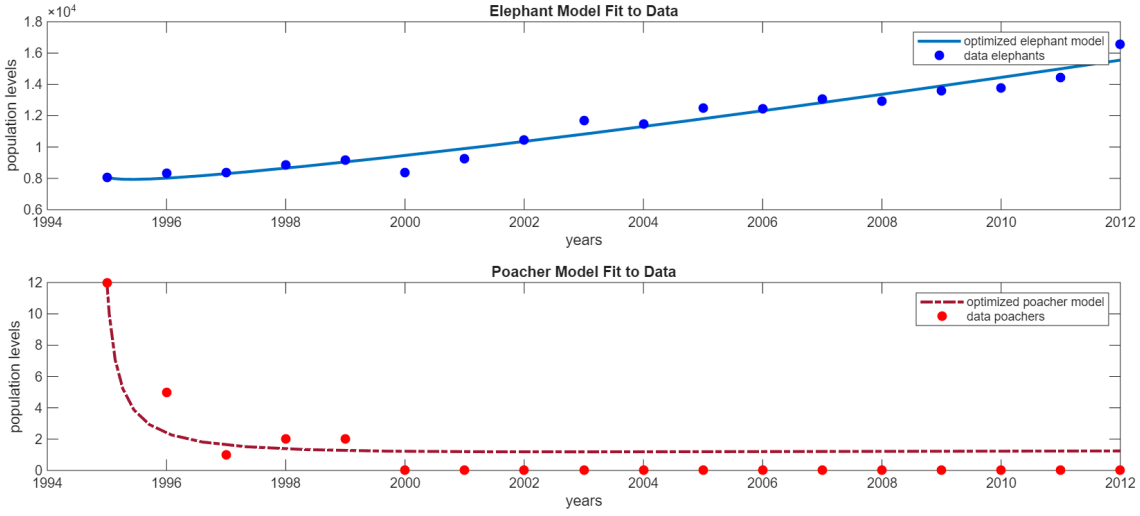

Figure 11: Best fit of the elephant and poacher models to data. The poacher data in the second subplot is inferred from the elephant population over the years.

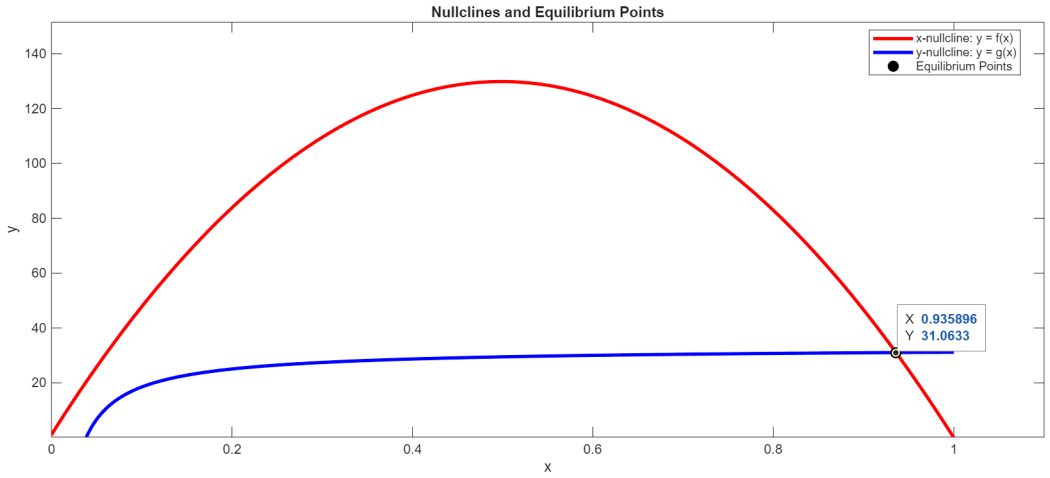

Figure 12: Plot of nullclines using dimensionless parameters from the best fit. Observe how the nontrivial x-nullcline given by $y = f(x)$ is decreasing at $x = x^*$. Then, by Theorem 3.6, (x^*, y^*) is locally stable. Here, $(x^*, y^*) \approx (0.936, 31.1)$.

As seen in Figure 12, there is only one biologically feasible coexistence equilibrium, and, by Theorem 3.6, it is locally stable. The available data suggest that, in the long run, protective efforts against poaching could allow the African elephant population in Kruger National Park to persist at approximately 93.6% of its carrying capacity. Furthermore, the approximate y^*-value of 31.1 suggests that, in the long run, the poacher population level would roughly be 1.3. In other words, despite current protective efforts, we would still expect for at least one African elephant to be poached annually. One reason for this outcome is that the estimated model parameters satisfy the condition $\delta - \mu a > \mu(1 + b^\nu)$. If additional protective efforts were implemented such that the condition $\delta - \mu a > \mu(1 + b^\nu)$ is no longer satisfied, then the resulting parameter regime would allow the African elephant population in Kruger National Park to approach its carrying capacity in the long run.

6. **Conclusion**

6.1. **Limitations of the model**

We were able to provide a mathematical analysis of our model and fit it to some available data. However, several limitations should be considered when interpreting our results. The primary limitation concerns data availability. We were unable to fully assess the performance of the model because some important data, such as the number of active poachers, are either unavailable or not readily accessible. A related limitation concerns the incorporation of the type IV functional response.

Our model assumes that humans protect groups of elephants, thereby representing a group-defense mechanism; however, data describing the extent and frequency of such protective behavior may be difficult, if not impossible, to obtain. Consequently, although the model is designed to capture biologically plausible behavior, the limited availability of empirical data makes it difficult to fully validate the model or use it to make reliable quantitative projections.

Another limitation is that the model does not account for changes in policies or regulations over time. In particular, we would ideally model the group-defense mechanism as a time-dependent process so that changes in restrictions, enforcement, and other conservation measures could be incorporated into the dynamics. Our current model effectively assumes that the same regulatory conditions remain in place throughout the entire time period under consideration. In reality, changes in laws and enforcement practices may influence both elephant and poacher population levels over time. Incorporating time-dependent policy parameters would therefore provide a natural extension of the model and could allow for a more realistic representation of the effects of conservation and anti-poaching efforts.

6.2. **Discussion and future work**

Throughout this work, we explored the mathematical modeling of elephant-poacher population dynamics. We established a theorem that guarantees the existence of at least one coexistence equilibrium, and identified a sufficient condition under which this equilibrium is locally stable. When we fitted our model to the data we had available, we found that it produced a locally stable coexistence equilibrium. A key implication of these results is that the African elephant population in Kruger National Park could persist at moderately high levels if current protective efforts continue, despite the continued presence of poaching threats. Ideally, continued efforts to protect endangered species could potentially lead to a sustained decline in poaching activity, eventually reducing the threat to a level at which African elephants can thrive in their natural environment.

Although substantial progress has been made in developing and analyzing this model, several directions for future work remain. First, additional mathematical analysis could be conducted to further characterize the graphical properties of the nontrivial x-nullcline, given by $y = f(x)$, including conditions governing its monotonicity and the existence and location of local extrema. Such an analysis would provide a more comprehensive understanding of the possible dynamics generated by the model. Second, as discussed in the limitations section, additional data on African elephant populations and poaching activity in Kruger National Park or other African

wildlife reserves could be obtained to improve the model fit and provide a more comprehensive assessment of strategies for reducing the poaching threat. In particular, such data could extend our initial efforts to estimate the number of active poachers at specific points in time by distinguishing elephant deaths resulting from natural causes from those resulting from poaching. Finally, future work could investigate ways to automate the parameter-search and model-fitting processes, which would facilitate more efficient analysis of additional datasets and parameter regimes.

References

[1] Elephant poaching: Why it's a big problem. *IFAW*, 2023.

[2] P. Blanchard, R.L. Devaney, and G.R. Hall. *Differential Equations*. Cengage Learning, 2012.

[3] F. Brauer and C. Castillo-Chávez. *Mathematical models in population biology and epidemiology*. Texts in applied mathematics ; 40. Springer, New York ;, 2nd [rev., updated and extended] ed. edition, 2012. Publication Title: Mathematical models in population biology and epidemiology.

[4] M.J. Chase, S. Schlossberg, C.R. Griffin, P.J.C. Bouché, S.W. Djene, P.W. Elkan, S. Ferreira, F. Grossman, E.M. Kohi, K. Landen, P. Omondi, A. Peltier, S.A.J. Selier, and R. Sutcliffe. Continent-wide survey reveals massive decline in african savannah elephants. *PeerJ*, 2016.

[5] B. Deng, S. Jessie, G. Ledder, A. Rand, and S. Srodulski. Biological control does not imply paradox. *Mathematical Biosciences*, 208(1):26–32, 2007.

[6] Poaching Facts. Elephant poaching statistics.

[7] J.W. Haefner. *Modeling biological systems : principles and applications*. Springer, New York, 2nd ed. edition, 2005. Publication Title: Modeling biological systems : principles and applications.

[8] M.C. Köhnke, I. Siekmann, H. Seno, and H. Malchow. A type iv functional response with different shapes in a predator–prey model. *Journal of Theoretical Biology*, 505, November 2020. Funding Information: The Japan Society for the Promotion of Science (JSPS) that provided funding for a stay at Tohoku University for MCK and HM supported this work. MCK acknowledge discussions with Frank M. Hilker about the bifurcation analysis. Publisher Copyright: © 2020 Elsevier Ltd.

[9] J.D. Logan. *Applied mathematics*. Wiley, Hoboken, New Jersey, fourth edition. edition, 2013. Publication Title: Applied mathematics.

[10] E. Líznarová and S. Pekár. Dangerous prey is associated with a type 4 functional response in spiders. *Animal Behaviour*, 85(6):1183–1190, 2013.

[11] B. Martin. *Survival or Extinction?: How to Save Elephants and Rhinos*. 01 2019.

[12] South African National Parks. Big trunks, bigger questions: Rethinking elephant numbers in kruger, 2025.

Theodora Schwallie
Department of Mathematics and Statistics, Haverford College, Haverford, PA
Email: theaschwallie@gmail.com

Lawrence Seminario-Romero
Department of Mathematics and Statistics, Haverford College, Haverford, PA
Email: lseminario@haverford.edu

© 2026 Schwallie, Seminario-Romero. This open-access article is licensed under CC BY 4.0.
Pittsburgh Interdiscip. Math. Rev. is managed by undergraduate students from the University of Pittsburgh and Carnegie Mellon University, and is published electronically through the University of Pittsburgh Library System.